unsaturated (and perhaps electrophilic) character of one partner may prove more general as further mechanistic information becomes available.

The facile exchange of alkyl groups in otherwise stable metal alkyls bodes caution for crossover experiments designed to probe the important mechanistic question of molecularity during reactions of those species. In extensions of the results outlined above, we have obtained preliminary evidence that alkyl exchange between transition-metal centers may be a more general process than has heretofore been suggested. Thus, although **1**-d_6 and Cp_2MoMe_2 do not exchange methyls, we *do* observe such exchange between **1**-d_6 and Cp_2ZrMe_2. Further research will be required to define more precisely the scope of these reactions, the factors which control their efficiency, and the nature of the exchange transition state.

Experimental Section

General. All manipulations of oxygen- or water-sensitive materials were conducted under a prescrubbed recirculating atmosphere of N_2 in a Vacuum Atmospheres HE-553 Dri-Lab with attached MO-40-1 Dri-Train or by using standard Schlenk or vacuum line techniques.

Tetrahydrofuran (THF) and diethyl ether were distilled from purple sodium/benzophenone ketyl solutions. Benzene and hexanes were degassed and used as supplied from J. T. Baker ("Analyzed Reagent" grade). PPh_3 (MCB) was recrystallized twice from hexanes and dried overnight under high vacuum. Methylcyclopentadiene was freshly distilled at atmospheric pressure from the commercially available (Aldrich) dimer and stored at −78 °C until used.

Infrared (IR) spectra were recorded on a Perkin-Elmer Model 283 grating spectrophotometer using solutions of samples in sodium chloride cells (0.10-mm path length).

Elemental analyses were conducted by the University of California, Berkeley analytical facility.

NMR Experiments. ^1H nuclear magnetic resonance (NMR) spectra were recorded on a Varian EM-390 spectrometer. Spectra are reported in units of ppm downfield from tetramethylsilane but were most often measured relative to residual ^1H absorption in deuterated solvent: benzene-d_6 (δ 7.15), THF-d_8 (δ 1.73), and acetone-d_6 (δ 2.04). Deuterated THF and benzene were vacuum transferred from ketyl solutions while acetone-d_6 was transferred from Linde 4A° molecular sieves and degassed with three freeze–pump–thaw cycles on a vacuum line.

NMR experiments were carried out as follows: a standard NMR tube fused to a 14/20 ground-glass joint was loaded with the desired compounds in the drybox, capped with a Teflon needle valve, placed on a vacuum line, and evacuated. The tube was charged with the desired amount of solvent by vacuum transfer from a graduated tube of solvent. The tube was then sealed and carefully thawed before being heated in a refluxing $CHCl_3$ bath. Spectra were recorded by removing the tube from the bath after the desired elapsed time, plunging it into ice water (none of the reactions proceeded at measurable rates below 55 °C), and placing it in the NMR probe when dry. The spectrum was recorded and the tube replaced in the constant temperature bath.

Syntheses. $CpCo(PPh_3)(CH_3)_2$, $CpCo(PPh_3)(CD_3)_2$, and $CpCo(P(CH_3)_3)(CD_3)_2$ were prepared by previously published methods.[6c] Methylcyclopentadienyl analogues were prepared by the same methods used to prepare the unsubstituted cyclopentadienyl complexes. Structures of previously known compounds were established by comparison of spectral data with those reported earlier; new compounds were characterized by standard spectral and analytical techniques. Data for new compounds follow: $(C_5H_4CH_3)Co(CO)I_2$: NMR ($CDCl_3/Me_4Si$) δ 5.42 (s, 4 H), 2.50 (s, 3 H); IR (Et_2O) 2065 cm^{-1}. Anal. Calcd for $C_7H_7CoI_2O$: C 20.02; H, 1.68; Co, 14.04; I, 60.45. Found: C, 20.22; H, 1.78; Co, 13.1; I, 60.48. $(C_5H_4CH_3)Co(PPh_3)I_2$: NMR ($CDCl_3/Me_4Si$) δ 7.2–7.9 (m, 15 H), 5.05 (m, AA′, 2 H), 4.15 (m, BB′, 2 H), 2.54 (d, J = 2.5 Hz, 3 H). Anal. Calcd for $C_{24}H_{22}CoI_2P$: C, 44.07; H, 3.39; Co, 9.01; I, 38.80; P, 4.73. Found: C, 43.85; H, 3.49; Co, 8.64; I, 39.02; P, 4.90. $(C_2H_4CH_3)Co(PPh_3)(CH_3)_2$: NMR (THF-$d_8$) δ 7.2–7.6 (m, 15 H), 5.1 (m, AA′BB′, 4 H), 1.58 (d, J = 3 Hz, 3 H), −0.05 (d, J = 5.5 Hz, 6 H). Anal. Calcd for $C_{26}H_{28}CoP$: C, 72.55; H, 6.56; Co, 13.69; P, 7.20. Found: C, 72.60; H, 6.55; Co, 14.0; P, 7.04. $(C_5H_4CH_3)Co(P(CH_3)_3)(CH_3)_2$: NMR (THF-$d_8$) δ 5.05, 5.30 (m, AA′BB′, 4 H), 2.35 (s, 3 H), 2.25 (d, J = 9 Hz, 9 H), 0.30 (d, J = 6 Hz, 6 H). High resolution MS: parent ion m/e calcd for $C_{11}H_{22}CoP$: 244.0799. Found: 244.0795.

Acknowledgments. We are grateful to Dr. F. A. Houle for assistance with the computer simulation, and we acknowledge financial support from the Division of Basic Energy Sciences, U.S. Department of Energy, under Contract No. W-7405-48.

Tautomeric Catecholate–Semiquinone Interconversion via Metal–Ligand Electron Transfer. Structural, Spectral, and Magnetic Properties of (3,5-Di-*tert*-butylcatecholato)(3,5-di-*tert*-butylsemiquinone)(bipyridyl)cobalt(III), a Complex Containing Mixed-Valence Organic Ligands

Robert M. Buchanan and Cortlandt G. Pierpont*

Contribution from the Department of Chemistry, University of Colorado, Boulder, Colorado 80309. *Received October 31, 1979*

Abstract: The bipyridyl adduct of tetrameric $[Co(3,5\text{-}DBSQ)_2]_4$ has been formed by treating the parent Co(II) complex with bipyridine in toluene solution. Structural features within the inner coordination sphere are consistent with a Co(III) metal center. One of the independent quinone ligands is coordinated as a semiquinone and the other as a catecholate. In toluene solution the results of magnetic, EPR, NMR, and spectral experiments suggest an equilibrium between a Co(II) species $Co(3,5\text{-}DBSQ)_2(bpy)$ and the Co(III) form found in the solid state, Co(3,5-DBCat)(3,5-DBSQ)(bpy). These two forms of the complex are related by the transfer of an electron between the metal ion and one of the quinone ligands.

Introduction

Mechanistic details of inner-sphere metal–ligand electron transfer, induced either thermally or photochemically, are of fundamental chemical importance but remain poorly understood.[1] Specific questions concern the nature of the ligand-radical species which is often the initial product of an outer-sphere electron-transfer process and the kinetics of the inner-sphere electron-transfer step.

Our studies on the coordination properties of orthoquinone ligands have shown that they are capable of chelating to metals as unreduced *o*-benzoquinones, as partially reduced *o*-semiquinones

---

(1) Tabue, H. "Electron Transfer Reactions of Complex Ions in Solution"; Academic Press: New York, 1970.

or as fully reduced catecholates (I).[2] The mode of coordination

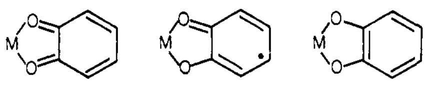

I

is directed by the nucleophilicity of the metal and the overall charge of the complex. We have examined the latter parameter in some detail, specifically for the tris(*o*-quinone)chromium complexes.[3] These undergo either chemical or electrochemical redox reactions which correspond to the addition or removal of charge from *ligand*-localized electronic levels by interaction with some external species (i.e., chemical agent, electrode surface). In this report we will consider intramolecular metal–ligand electron transfer within the complex unit. The various bonding descriptions shown above can be induced intramolecularly by transfer of one or two electrons between the metal and the π^* level of the quinone. Photolytic metal to ligand electron transfer is known for diimine complexes and plays a central role in their utility as sensitizers in energy-transfer processes.[4] In this report we will describe a reversible semiquinone–catecholate interconversion which is thermally induced and involves electron transfer to and from a cobalt center.

Experimental Section

(3,5-Di-*tert*-butylcatecholato)(3,5-di-*tert*-butylsemiquinone)(2,2′-bipyridyl)cobalt(III). A solution containing 0.20 g (0.1 mmol) of the bis(3,5-di-*tert*-butylsemiquinone)cobalt(II) tetramer dissolved in 50 mL of toluene was treated under an atmosphere of N_2 with 0.06 g (0.4 mmol) of 2,2′-bipyridine dissolved in 15 mL of toluene. The solution rapidly turned from the dark blue-green of the tetramer to the blue-black of the bipyridine adduct. Evaporation of the solvent produced 0.16 g of crystalline $Co(O_2C_6H_2(t\text{-}Bu)_2)_2(C_{10}H_8N_2)$, isolated as a toluene solvate.

Molecular Structure Determination of Co(3,5-DBCat)(3,5-DBSQ)(bpy)·0.5$C_6H_5CH_3$. Preliminary photographs taken on crystals obtained by using the synthetic procedure above indicated monoclinic symmetry. Systematic absences indicated space group *C*2/*c*. The nonstandard setting *I*2/*a* given in Table I was chosen for data collection and the structure determination so as to give the least obtuse unit cell.[6] A crystal of dimensions 0.36 × 0.42 × 0.56 mm was mounted and aligned on a Syntex P$\bar{1}$ automated diffractometer. The settings of 15 high angle reflections were used to calculate the refined cell constants given in Table I. Data were collected by the θ–2θ scan technique with four standard reflections measured periodically throughout data collection. No significant variation in intensity was observed for the standards, and data were processed in the usual way. The crystal structure was solved by using standard heavy-atom procedures. The location of the cobalt atom was determined from a Patterson function, and phases from the refinement of the cobalt atom were used to find other atoms of the complex molecule. Rotational disorder was found for one *tert*-butyl group of the catecholate ligand. The difference Fourier map calculated from a cycle of isotropic refinement of the entire complex molecule showed that the toluene solvate molecule was disordered along the twofold axis of the space group. The solvate molecule was found to lie perpendicular to the twofold axis with the axis passing through one carbon–carbon bond of the ring giving a naphthalene-like species. Two possible locations were found for the toluene methyl carbon. Final cycles of refinement converged with $R_F = 0.076$ and $R_{wF} = 0.083$ for 2647 independent reflections. The final difference Fourier map showed features which were approximately 0.15 the height of a carbon atom in the vicinity of the disordered toluene solvate. Sources of scattering factor tables, computer programs, and calculational procedures have been noted.[7] The value of the standard deviation of an observation of unit weight was 1.90. Final positional and thermal parameters for $Co(O_2C_6H_2(t\text{-}Bu)_2)_2(C_{10}H_8N_2)\cdot 0.5C_6H_5CH_3$ are listed in Table II. Values for $10|F_o|$ and $10|F_c|$ (in electrons) are available as supplementary material.

Table I. Crystallographic Data for Co(3,5-DBCat)(3,5-DBSQ)(bpy)·0.5$C_6H_5CH_3$

fw: 702.09	$d(\text{calcd}) = 1.084$ g cm^{-3}
monoclinic	$d(\text{exptl}) = 1.08$ (1) g cm^{-3}
space group *I*2/*a*	$Z = 8$
$a = 34.776$ (7) Å	$\mu = 4.29$ cm^{-1}
$b = 14.798$ (2) Å	scan rate: 4°/min
$c = 16.719$ (2) Å	2θ limits: $3° \leqslant \theta \leqslant 45°$
$\beta = 90.92$ (1)°	scan range: ±0.7°
$V = 8602$ (2) Å^3	data measd: 5945
Mo Kα ($\bar{\lambda} = 0.710\ 73$ Å)	data $F_o^2 > 3\sigma(F_o^2)$: 2647

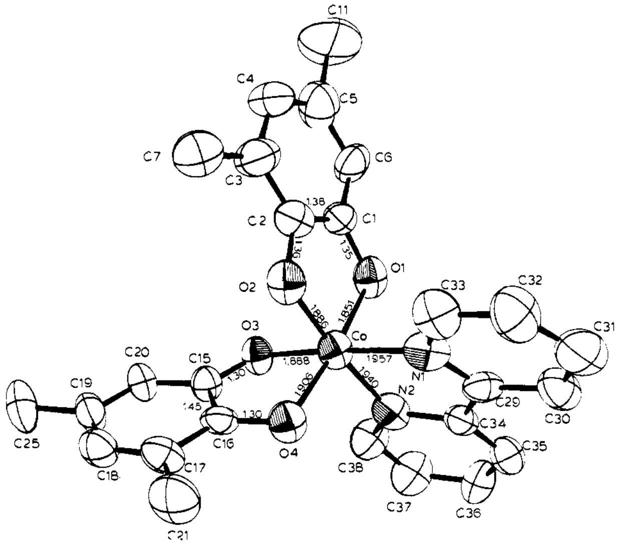

Figure 1. View of the $Co(O_2C_6H_2(t\text{-}Bu)_2)_2(bpy)$ molecule showing the atom-numbering scheme and bond distances within the inner coordination sphere.

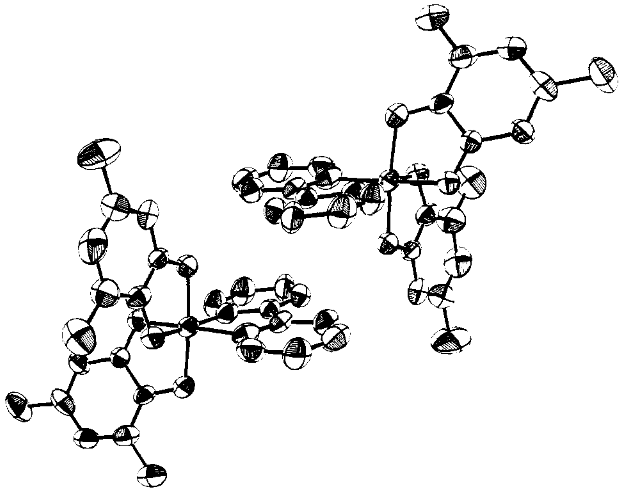

Figure 2. View showing the weak pairing of $Co(O_2C_6H_2(t\text{-}Bu)_2)_2(bpy)$ molecules within the unit cell. The separation between adjacent bipyridyl ligands is 3.65 Å, and, as shown in Table IV, the ligand is essentially planar.

Physical Measurements. Electronic spectra were recorded either as Nujol mulls or in toluene solution on Cary 219 and Cary 17 spectrophotometers. NMR spectra were recorded either on a Varian EM-390 at the University of Colorado or on a JEOL FX-100 Fourier transform spectrometer at the Regional NMR Center at Colorado State University. EPR spectra were recorded on a Varian E-9 spectrometer at the University of Denver.

Results and Discussion

Description of the $Co(O_2C_6H_2(t\text{-}Bu)_2)_2(bpy)$ Molecule. A view of the $Co(O_2C_6H_2(t\text{-}Bu)_2)_2(bpy)$ molecule showing the atom la-

---

[2] Buchanan, R. M.; Kessel, S. L.; Downs, H. H.; Pierpont, C. G.; Hendrickson, D. N. *J. Am. Chem. Soc.* **1978**, *100*, 7894.

[3] Downs, H. H.; Buchanan, R. M.; Pierpont, C. G. *Inorg. Chem.* **1979**, *18*, 1736.

[4] (a) Meyer, T. J. *Acc. Chem. Res.* **1978**, *11*, 94. (b) Balzani, V.; Bolletta, F.; Gandolfi, M. T.; Maestri, M. *Top. Curr. Chem.* **1978**, *75*, 1. (c) Bock, C. R.; Connor, J. A.; Gutierrez, A. R.; Meyer, T. J.; Whitten, D. G.; Sullivan, B. P.; Nagle, J. K. *J. Am. Chem. Soc.* **1979**, *101*, 4815.

[5] Buchanan, R. M.; Fitzgerald, B. J.; Pierpont, C. G. *Inorg. Chem.* **1979**, *18*, 3439.

[6] Unit cell dimensions in *C*2/*c* are $a = 38.313$ (7) Å, $b = 14.798$ (2) Å, $c = 16.719$ (2) Å, and $\beta = 114.78$ (1)°.

[7] Pierpont, C. G. *Inorg. Chem.* **1977**, *16*, 636.

[8] Bertrand, J. A.; Fujita, E.; Van Derveer, D. G. *Inorg. Chem.* **1979**, *18*, 230.

Table II. Positional and Thermal Parameters for the Atoms of Co(3,5-DBCat)(3,5-DBSQ)(bpy)·$0.5C_6H_5CH_3$

atom	x	y	z	B_{11}[a]	B_{22}	B_{33}	B_{12}	B_{13}	B_{23}
Co	0.16553 (4)	0.15429 (9)	0.14683 (7)	4.52 (7)	4.27 (7)	2.86 (6)	−0.73 (7)	0.50 (4)	0.05 (6)
O(1)	0.1849 (2)	0.2689 (4)	0.1207 (3)	4.5 (4)	5.0 (4)	3.2 (3)	−1.3 (3)	0.1 (3)	0.2 (3)
O(2)	0.1169 (2)	0.2037 (5)	0.1375 (3)	4.7 (4)	5.1 (4)	4.0 (3)	−1.2 (3)	0.2 (3)	0.4 (3)
C(1)	0.1552 (3)	0.3238 (6)	0.1004 (5)	4.8 (6)	3.0 (6)	2.7 (4)	−0.2 (5)	0.0 (4)	0.3 (4)
C(2)	0.1189 (3)	0.2890 (7)	0.1082 (5)	5.5 (7)	3.9 (6)	3.4 (5)	0.0 (5)	0.7 (5)	0.2 (4)
C(3)	0.0874 (3)	0.3405 (8)	0.0856 (6)	4.8 (5)	4.8 (7)	7.8 (6)	0.6 (6)	−0.6 (5)	0.7 (5)
C(4)	0.0948 (4)	0.4283 (8)	0.0556 (7)	8.3 (5)	4.7 (8)	7.2 (7)	2.2 (8)	−1.6 (7)	−0.2 (6)
C(5)	0.1315 (4)	0.4607 (8)	0.0496 (6)	7.1 (5)	5.9 (8)	6.5 (7)	−1.7 (6)	−0.9 (7)	0.5 (6)
C(6)	0.1619 (3)	0.4084 (7)	0.0723 (5)	5.1 (5)	5.5 (7)	3.7 (7)	0.4 (6)	−0.9 (5)	0.5 (6)
C(7)	0.0464 (3)	0.3034 (8)	0.0898 (8)	6.6 (8)	6.9 (8)	9.5 (10)	1.4 (9)	−0.8 (6)	−1.1 (7)
C(8)	0.0384 (3)	0.2713 (10)	0.1740 (8)	6.6 (8)	13.8 (7)	8.9 (9)	0.1 (9)	2.6 (6)	−0.5 (7)
C(9)	0.0424 (3)	0.2227 (11)	0.0331 (8)	4.6 (8)	14.6 (10)	10.9 (9)	−2.1 (8)	−0.1 (7)	0.3 (8)
C(10)	0.0161 (4)	0.3696 (10)	0.0633 (12)	4.8 (7)	10.0 (11)	30.6 (9)	2.0 (8)	−2.5 (6)	2.5 (7)
C(11)	0.1368 (5)	0.5595 (9)	0.0152 (10)	13.8 (8)	4.8 (11)	13.2 (15)	−0.6 (8)	−0.4 (9)	3.3 (12)
C(12)[b]	0.0958 (11)	0.6014 (22)	−0.0018 (35)	14 (4)	3 (3)	31 (8)	0 (2)	−11 (5)	6 (3)
C(13)[b]	0.1617 (11)	0.5434 (19)	−0.0577 (19)	14 (3)	7 (3)	9 (3)	−2 (2)	−0 (2)	6 (2)
C(14)[b]	0.1577 (12)	0.6115 (16)	0.0837 (20)	13 (3)	3 (2)	13 (3)	−3 (2)	−3 (2)	0 (2)
C(12)A[b]	0.1790 (10)	0.5812 (26)	0.0042 (47)	11 (3)	7 (4)	39 (8)	−4 (2)	3 (5)	10 (5)
C(13)A[b]	0.1239 (25)	0.5550 (28)	−0.0769 (23)	32 (8)	11 (4)	9 (2)	−2 (6)	−11 (5)	9 (3)
C(14)A[b]	0.1142 (18)	0.6300 (18)	0.0517 (33)	28 (5)	2 (2)	28 (7)	−3 (4)	13 (7)	−4 (3)
O(3)	0.1626 (2)	0.1225 (4)	0.0375 (3)	4.2 (3)	4.5 (4)	3.2 (3)	−0.9 (3)	0.1 (2)	−0.2 (2)
O(4)	0.1418 (2)	0.0407 (4)	0.1650 (4)	5.0 (4)	4.9 (4)	3.3 (3)	−0.8 (3)	0.3 (3)	0.4 (3)
C(15)	0.1372 (3)	0.0594 (7)	0.0281 (5)	3.7 (5)	4.0 (5)	3.1 (5)	−0.5 (4)	0.1 (4)	0.0 (4)
C(16)	0.1245 (3)	0.0145 (6)	0.0997 (6)	4.6 (6)	2.5 (5)	3.9 (5)	0.1 (4)	0.1 (4)	0.8 (4)
C(17)	0.0967 (3)	−0.0551 (7)	0.0939 (6)	5.9 (5)	3.6 (5)	4.9 (6)	−0.5 (4)	0.9 (4)	0.3 (4)
C(18)	0.0822 (3)	−0.0760 (6)	0.0208 (6)	5.2 (5)	4.0 (6)	5.3 (7)	−1.2 (4)	0.3 (5)	0.4 (5)
C(19)	0.0953 (3)	−0.0332 (7)	−0.0514 (6)	4.3 (6)	4.5 (6)	6.7 (6)	−0.4 (4)	−0.9 (5)	−2.0 (5)
C(20)	0.1217 (3)	0.0327 (6)	−0.0470 (5)	4.0 (7)	4.3 (5)	4.6 (6)	−1.1 (4)	−0.3 (5)	−1.6 (5)
C(21)	0.0825 (3)	−0.1011 (7)	0.1700 (7)	7.0 (8)	5.8 (7)	6.7 (7)	−1.6 (6)	0.8 (7)	1.2 (6)
C(22)	0.1161 (4)	−0.1523 (9)	0.2115 (7)	10.5 (8)	8.1 (9)	8.5 (8)	−1.5 (6)	0.3 (7)	4.5 (7)
C(23)	0.0514 (4)	−0.1678 (9)	0.1525 (8)	10.0 (9)	8.9 (8)	12.6 (8)	−6.1 (8)	0.8 (7)	1.6 (7)
C(24)	0.0659 (3)	−0.0300 (9)	0.2265 (7)	7.6 (9)	9.7 (9)	7.9 (9)	−1.2 (8)	3.7 (7)	2.0 (8)
C(25)	0.0766 (3)	−0.0587 (8)	−0.1339 (7)	7.1 (9)	8.0 (10)	6.7 (8)	−2.0 (6)	−1.3 (5)	−2.8 (7)
C(26)	0.0943 (4)	−0.0144 (13)	−0.2024 (7)	12.8 (10)	23 (2)	4.9 (10)	−10.6 (10)	−0.9 (9)	−2.4 (8)
C(27)	0.0765 (5)	−0.1596 (11)	−0.1454 (8)	20.8 (10)	9 (2)	9.7 (10)	−1.9 (10)	−4.5 (8)	−4.8 (8)
C(28)	0.0336 (4)	−0.0306 (12)	−0.1314 (9)	9.0 (10)	20.3 (2)	9.8 (10)	2.0 (10)	−4.2 (7)	−2.7 (10)
N(1)	0.1712 (2)	0.1793 (5)	0.2614 (4)	4.6 (4)	4.2 (4)	4.1 (4)	0.2 (3)	1.6 (3)	0.3 (3)
C(29)	0.2066 (3)	0.1665 (6)	0.2905 (5)	4.3 (5)	3.0 (5)	3.3 (4)	0.6 (4)	0.6 (4)	0.6 (4)
C(30)	0.2152 (3)	0.1878 (6)	0.3691 (5)	6.6 (5)	4.2 (5)	3.5 (4)	−0.1 (4)	0.6 (4)	−0.6 (4)
C(31)	0.1865 (3)	0.2212 (7)	0.4189 (6)	8.0 (7)	4.7 (6)	4.3 (6)	−0.2 (6)	0.8 (5)	0.4 (5)
C(32)	0.1494 (3)	0.2297 (7)	0.3871 (6)	7.6 (7)	6.8 (7)	3.8 (6)	−0.3 (6)	1.2 (5)	−1.0 (5)
C(33)	0.1423 (3)	0.2104 (7)	0.3065 (6)	5.1 (6)	5.6 (6)	5.3 (7)	−1.2 (5)	1.0 (5)	0.0 (5)
N(2)	0.2177 (2)	0.1118 (5)	0.1630 (4)	5.1 (4)	4.1 (4)	3.2 (3)	−0.5 (3)	0.8 (3)	0.1 (3)
C(34)	0.2334 (2)	0.1294 (5)	0.2359 (5)	4.0 (5)	2.7 (5)	3.2 (4)	0.0 (4)	0.2 (4)	0.0 (4)
C(35)	0.2714 (3)	0.1119 (6)	0.2536 (5)	4.5 (6)	4.3 (5)	3.2 (4)	−0.2 (4)	0.5 (4)	−0.8 (4)
C(36)	0.2931 (3)	0.0731 (7)	0.1959 (6)	5.5 (7)	7.1 (7)	3.7 (6)	−0.2 (5)	−1.0 (5)	0.4 (5)
C(37)	0.2776 (3)	0.0541 (8)	0.1223 (6)	5.3 (7)	7.8 (7)	4.6 (6)	0.6 (6)	0.8 (5)	0.0 (5)
C(38)	0.2401 (3)	0.0744 (7)	0.1064 (5)	4.8 (8)	6.4 (6)	3.6 (4)	0.7 (5)	0.5 (4)	−0.2 (4)

	x	y	z	B, Å^2		x	y	z	B, Å^2
TC(1)[b]	0.2354 (31)	−0.1637 (18)	0.0204 (22)	4 (3)	TC(5)[b]	0.2950 (21)	−0.1875 (30)	0.0990 (18)	7 (3)
TC(2)[b]	0.2955 (23)	−0.1574 (26)	0.0192 (34)	9 (2)	TC(6)[c]	0.2514 (30)	−0.1498 (32)	0.2750 (37)	15 (6)
TC(3)[b]	0.2868 (28)	−0.1459 (28)	−0.0925 (28)	7 (2)	TC(7)[c]	0.2784 (38)	−0.2274 (36)	0.2283 (40)	15 (6)
TC(4)[b]	0.2462 (16)	−0.1761 (26)	−0.1115 (26)	9 (4)					

[a] The form of the anisotropic thermal ellipsoid is $\exp[-0.25(B_{11}h^2a^{*2} + B_{22}k^2b^{*2} + B_{33}l^2c^{*2} + 2B_{12}hka^*b^* + 2B_{13}hla^*c^* + 2B_{23}kl_2b^*c^*)]$ and is given in units of Å.^{2} [b] Atom refined with an occupancy factor of 0.50. [c] Atom refined with an occupancy factor of 0.25.

beling scheme is given in Figure 1. Intramolecular bond distances and angles are contained in Table III. The crystal structure consists of weakly coupled pairs of complex molecules located about crystallographic centers of inversion. This interaction results from overlap of adjacent bipyridyl ligands as shown in Figure 2. The interplanar separation between adjacent bipyridyl rings is approximately 3.65 Å which is relatively long for stacked aromatic molecules. The disordered toluene solvate molecule is well separated from the complex.

Synthetically, $Co(O_2C_6H_2(t\text{-}Bu)_2)_2(bpy)$ is formed by treating the cobalt(II)–semiquinone complex Co_4(3,5-DBSQ)$_8$ with bipyridyl. A Co(II) product, Co(3,5-DBSQ)$_2$(bpy), might be expected from this reaction; however, $Co(O_2C_6H_2(t\text{-}Bu)_2)_2(bpy)$ shows structural features which suggest Co(III). Cobalt–oxygen lengths range from 1.851 (6) to 1.906 (6) Å with the longest and shortest values to the trans oxygen atoms O(1) and O(4). The bipyridyl ligand of the adjacent molecule is located on the O(4) side of the view shown in Figure 1 and may contribute to the lengthening of the Co–O(4) bond. Cobalt–nitrogen lengths to the bipyridyl ligand are 1.940 (7) and 1.957 (7) Å for N(2) and N(1). The mixed-valence Co(II)–Co(III) complex $Co_4(NH(C_2H_4OH)_2)_2NH(C_2H_4O)_2)_4{}^{2+}$, prepared and characterized structurally by Bertrand and co-workers,[8] shows the expected structural differences between high-spin Co(II) and Co(III) as reflected in Co–O and Co–N bond lengths within the inner coordination sphere. In this tetranuclear cation Co(III)–O lengths range from 1.888 (3) to 1.940 (3) Å while Co(II)–O values vary from 2.045 (3) to 2.225 (3) Å. As a general result Co(II)–O lengths exceed 2.00 Å. In the cobalt(II)–semiquinone complex, Co_4(3,5-DBSQ)$_8$,[5] used in the synthesis of the present compound Co–O lengths range from 2.020 (4) to 2.175 (4) Å. Cobalt–nitrogen lengths show a similar pattern with Co(II) values approximately 0.1 Å longer than values found in related Co(III) compounds. Bertrand's cation has Co(III)–N lengths of 1.957

Table III. Bonding Parameters for the Co(3,5-DBCat)(3,5-DBSQ)(bpy) Complex Molecule

	Inner Coordination Sphere (Å)		
Co–O(1)	1.851 (6)	Co–O(4)	1.906 (6)
Co–O(2)	1.886 (6)	Co–N(1)	1.957 (7)
Co–O(3)	1.888 (6)	Co–N(2)	1.940 (7)
	Angles (Deg)		
O(1)–Co–O(2)	87.4 (3)	O(2)–Co–N(2)	174.7 (3)
O(1)–Co–O(3)	90.8 (2)	O(3)–Co–O(4)	85.3 (3)
O(1)–Co–O(4)	173.9 (3)	O(3)–Co–N(1)	175.5 (3)
O(1)–Co–N(1)	91.5 (3)	O(3)–Co–N(2)	95.0 (3)
O(1)–Co–N(2)	89.3 (3)	O(4)–Co–N(1)	92.8 (3)
O(2)–Co–O(3)	89.1 (3)	O(4)–Co–N(2)	95.6 (3)
O(2)–Co–O(4)	88.0 (3)	N(1)–Co–N(2)	81.2 (3)
O(2)–Co–N(1)	94.8 (3)		
	Catecholate Ligand (Å)		
O(1)–C(1)	1.354 (10)	C(4)–C(5)	1.372 (14)
O(2)–C(2)	1.362 (10)	C(5)–C(6)	1.361 (13)
C(1)–C(2)	1.376 (12)	C(6)–C(1)	1.364 (12)
C(2)–C(3)	1.383 (12)	C(3)–C(7)	1.536 (14)
C(3)–C(4)	1.422 (14)	C(5)–C(11)	1.588 (15)
	Angles (Deg)		
Co–O(1)–C(1)	109.0 (5)	C(3)–C(4)–C(5)	121.5 (10)
Co–O(2)–C(2)	110.2 (6)	C(4)–C(5)–C(6)	120.0 (11)
O(1)–C(1)–C(2)	116.8 (8)	C(5)–C(6)–C(1)	119.1 (12)
O(1)–C(1)–C(6)	120.5 (10)	C(6)–C(1)–C(2)	122.8 (10)
O(2)–C(2)–C(1)	115.9 (9)	C(2)–C(3)–C(7)	121.6 (11)
O(2)–C(2)–C(3)	124.5 (10)	C(4)–C(3)–C(7)	121.3 (11)
C(1)–C(2)–C(3)	119.6 (10)	C(4)–C(5)–C(11)	117.8 (12)
C(2)–C(3)–C(4)	117.1 (10)	C(6)–C(5)–C(11)	122.3 (12)
	Semiquinone Ligand (Å)		
O(3)–C(15)	1.297 (9)	C(18)–C(19)	1.446 (12)
O(4)–C(16)	1.297 (9)	C(19)–C(20)	1.345 (11)
C(15)–C(16)	1.446 (11)	C(15)–C(20)	1.414 (11)
C(16)–C(17)	1.420 (12)	C(17)–C(21)	1.532 (12)
C(17)–C(18)	1.350 (11)	C(19)–C(25)	1.560 (13)
	Angles (Deg)		
Co–O(3)–C(15)	108.8 (5)	C(17)–C(18)–C(19)	122.4 (9)
Co–O(4)–C(16)	109.0 (5)	C(18)–C(19)–C(20)	120.1 (9)
O(3)–C(15)–C(16)	116.8 (8)	C(19)–C(20)–C(15)	120.1 (9)
O(3)–C(15)–C(20)	124.0 (8)	C(16)–C(15)–C(20)	119.2 (9)
O(4)–C(16)–C(15)	114.5 (8)	C(16)–C(17)–C(21)	119.8 (9)
O(4)–C(16)–C(17)	125.5 (8)	C(18)–C(17)–C(21)	121.9 (10)
C(15)–C(16)–C(17)	119.9 (9)	C(18)–C(19)–C(25)	119.8 (9)
C(16)–C(17)–C(18)	118.2 (9)	C(20)–C(19)–C(25)	120.0 (10)
	Bipyridyl Ligand (Å)		
N(1)–C(29)	1.329 (10)	C(34)–C(35)	1.377 (11)
N(2)–C(34)	1.352 (9)	C(35)–C(36)	1.363 (12)
C(29)–C(30)	1.379 (11)	C(36)–C(37)	1.364 (12)
C(30)–C(31)	1.403 (12)	C(37)–C(38)	1.360 (12)
C(31)–C(32)	1.393 (13)	N(2)–C(38)	1.356 (10)
C(32)–C(33)	1.396 (12)	C(29)–C(34)	1.430 (10)
N(1)–C(33)	1.351 (10)		
	Angles (Deg)		
Co–N(1)–C(29)	114.1 (5)	C(34)–N(2)–C(38)	118.7 (8)
Co–N(2)–C(34)	115.1 (5)	N(2)–C(34)–C(35)	121.9 (8)
Co–N(1)–C(33)	123.2 (5)	C(34)–C(35)–C(36)	118.0 (8)
Co–N(2)–C(38)	125.9 (5)	C(35)–C(36)–C(37)	120.7 (10)
C(29)–N(1)–C(33)	122.6 (8)	C(36)–C(37)–C(38)	119.5 (10)
C(30)–C(29)–N(1)	120.0 (8)	C(37)–C(38)–N(2)	121.1 (9)
C(29)–C(30)–C(31)	120.1 (10)	N(1)–C(29)–C(34)	115.7 (8)
C(30)–C(31)–C(32)	118.1 (9)	C(30)–C(29)–C(34)	124.3 (9)
C(31)–C(32)–C(33)	119.7 (10)	N(2)–C(34)–C(29)	113.1 (8)
C(32)–C(33)–N(1)	119.3 (10)	C(29)–C(34)–C(35)	125.0 (8)

(4) and 1.968 (4) Å, while the single unique Co(II)–N length was found to be 2.241 (4) Å. Therefore, the ligand bond lengths of $Co(O_2C_6H_2(t\text{-}Bu)_2)_2(bpy)$ appear to indicate Co(III) requiring either a delocalized electron distribution between the two quinone ligands or a localized structure with one ligand coordinated as a catecholate and the other as a semiquinone. Surprisingly, features of the ligands indicate the latter. While structural differences between chelated semiquinone and catecholate ligands are relatively small, there are consistent differences which have appeared for a large number of independent ligands in several structure determinations on complexes of semiquinones.[2,5,9] In Table V the average C–O lengths of semiquinone ligands are compared with a few representative catecholate complexes. As we have noted previously, carbon–oxygen lengths of semiquinones show little variation from the value of 1.29 (1) Å while chelated catecholates generally are found to have values close to 1.35 (1) Å. In $Co(O_2C_6H_2(t\text{-}Bu)_2)_2(bpy)$ C–O lengths of 1.354 (10) and 1.362 (10) Å are found for the ligand containing O(1) and O(2) while values of 1.297 (9) Å are found to O(3) and O(4). These values point to a localized catecholate–semiquinone electronic structure for the two independent ligands. A small but consistent difference in the carbon–carbon length between quinone carbon atoms within the chelate ring is found for the two types of ligands. This value is typically 1.44 (1) Å for semiquinones, slightly longer than the aromatic value of 1.39 (1) for catecholates. In the present molecule the C(1)–C(2) length is 1.376 (12) Å while the C(15)–C(16) length is 1.446 (11) Å. A further difference between semiquinone and catecholate ligands which appears in the comparison of tris(9,10-phenanthrenesemiquinone)iron(III) with the tris(catecholato)iron(III) trianion and tris(tetrachloro-*o*-semiquinone)chromium(III) with the tris(catecholato)chromium(III) trianion is that the ligand bite angle of the semiquinone is typically 2° smaller than that of the catecholate ligand.[2] This is also observed in $Co(O_2C_6H_2(t\text{-}Bu)_2)_2(bpy)$ where the O(3)–Co–O(4) angle is found to be 85.3 (3)° while the O(1)–Co–O(2) angle is 87.4 (3)°. The bipyridyl ligand could potentially be involved with charge delocalization; however, the short N(1)–C(29) and N(2)–C(34) lengths (1.329 (10), 1.352 (9) Å) within the chelate ring and long C(29)–C(34) length (1.430 (10) Å) appear to indicate normal bipyridyl coordination.

Table IV. Least-Squares Planes for the Ligands of Co(3,5-DBCat)(3,5-DBSQ)(bpy)

atom	dev, Å	atom	dev, Å
	Plane 1, Catecholate Ligand		
	$1.85x - 5.39y - 15.57z = 3.01$		
O(1)	0.022 (5)	C(5)	−0.005 (11)
O(2)	−0.014 (6)	C(6)	−0.020 (9)
C(1)	−0.013 (8)	C(7)	0.061 (13)
C(2)	−0.014 (8)	C(11)	0.009 (13)
C(3)	0.002 (10)	Co	0.20
C(4)	0.009 (11)		
	Plane 2, Semiquinone Ligand		
	$25.26x - 10.11y - 2.00z = -2.81$		
O(3)	−0.019 (6)	C(19)	0.032 (9)
O(4)	0.026 (6)	C(20)	0.025 (9)
C(15)	−0.004 (9)	C(21)	−0.047 (12)
C(16)	−0.015 (9)	C(25)	−0.018 (13)
C(17)	−0.002 (9)	Co	−0.49
C(18)	−0.010 (10)		
	Plane 3, Bipyridyl Ligand		
	$8.83x + 13.72y - 4.90z = -2.65$		
N(1)	0.037 (7)	N(2)	0.003 (7)
C(29)	0.031 (9)	C(34)	0.027 (8)
C(30)	0.015 (9)	C(35)	0.035 (9)
C(31)	−0.024 (10)	C(36)	−0.023 (10)
C(32)	−0.079 (11)	C(37)	−0.060 (11)
C(33)	−0.012 (10)	C(38)	−0.035 (10)
		Co	0.04

With the localized catecholate–semiquinone structure there are four possible structural isomers, two cis and two trans. The neutral Cr(III) complex $Cr(3,5\text{-}DBSQ)_3$ characterized structurally by Raymond[9] was found to form as the cis isomer, and the geometry of Co(3,5-DBCat)(3,5-DBSQ)(bpy) is also found to have the *tert*-butyl substituents at the 3 position of the ligand ring oriented

---

(9) Sofen, S. R.; Ware, D. C.; Cooper, S. R.; Raymond, K. N. *Inorg. Chem.* **1979**, *18*, 234.

Table V. Average Carbon–Oxygen and Carbon–Carbon Lengths for Semiquinone and Catecholate Chelate Rings

semiquinone complexes				catecholate complexes			
	C–O	C–C	ref		C–O	C–C	ref
$Fe(phenSQ)_3$	1.283 (3)	1.435 (6)	2	$Fe(Cat)_3^{3-}$	1.349 (3)	1.409 (4)	*b*
$Cr(o\text{-}Cl_4SQ)_3$	1.28 (1)	1.44 (1)	*a*	$Cr(Cat)_3^{3-}$	1.349 (3)	1.411 (4)	*b*
$Cr(3,5\text{-}DBSQ)_3$	1.285 (8)	1.433 (9)	9	$Mo_2(o\text{-}Cl_4Cat)_6$	1.342 (10)	1.380 (10)	*c*
$[Co(3,5\text{-}DBSQ)_2]_4$	1.285 (11)	1.448 (7)	5	$U(Cat)_4^{4-}$	1.349 (6)	1.407 (7)	*d*
Co(3,5-DBCat)(3,5-DBSQ)(bpy)	1.297 (9)	1.446 (11)		Co(3,5-DBCat)(3,5-DBSQ)(bpy)	1.358 (10)	1.376 (12)	

[a] Pierpont, C. G.; Downs, H. H. *J. Am Chem. Soc.* 1976, *98*, 4834. [b] Raymond, K. N.; Isied, S. S.; Brown, L. D.; Fronczek, F. F.; Nibert, J. H. *Ibid.* 1976, *98*, 1767. [c] Pierpont, C. G.; Downs, H. H. *Ibid.* 1975, *97*, 2123. [d] Sofen, S. R.; Abu-Dari, K.; Freyberg, D. P.; Raymond, K. N. *Ibid.* 1978, *100*, 7882.

toward a common triangular face of the octahedron. There are two structural isomers for this complex, IIa,b related by exchange of an electron between the two ligands. In our present determination we find isomer IIa and its related enantiomer. This result prompted further investigation of the complex to determine whether intramolecular electron transfer between the two nominally equivalent quinone ligands could be observed to occur in solution.

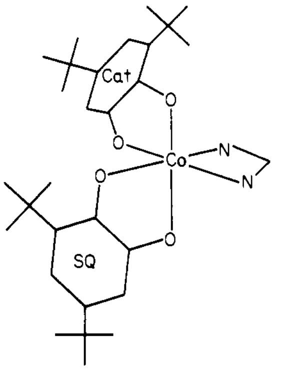

IIa

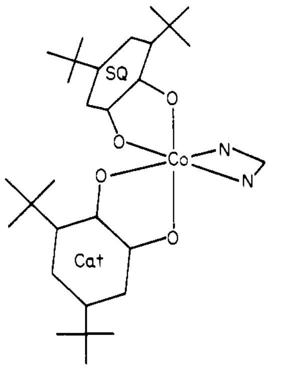

IIb

Magnetic Properties of $Co(O_2C_6H_2(t\text{-}Bu)_2)_2(bpy)$. A room-temperature magnetic susceptibility determination was carried out on a crystalline sample of $Co(O_2C_6H_2(t\text{-}Bu)_2)_2{\cdot}0.5C_6H_5CH_3$. The value obtained was 1.92 μ_B, approximately the value expected for an $S = {}^1/_2$ molecule. This agrees with the result of the structure determination which indicated a diamagnetic Co(III) metal center with a single $S = {}^1/_2$ semiquinone ligand. Magnetic susceptibility determinations carried out in toluene solution produced quite different results. The room-temperature magnetic moment was found to be 3.75 μ_B, considerably larger than the solid-state moment. Additional determinations measured over the temperature range from −67 to +77 °C indicated the temperature dependence shown in Figure 3. At low temperature the limiting moment approaches the solid-state value. At higher temperatures a value of 4.26 μ_B (60 °C) was observed. In an earlier report we noted that the parent Co(II) complex $[Co(O_2C_6H_2(t\text{-}Bu)_2)_2]_4$ with semiquinone ligands exhibits a room-temperature magnetic moment of 4.75 μ_B/cobalt center.[5] This is due to weak antiferromagnetic exchange between the $S = {}^3/_2$ metal center and the two $S = {}^1/_2$ ligands per monomeric unit. Subsequent variable-temperature magnetic susceptibility determinations have confirmed this conclusion.[10] The higher temperature magnetic moment of $Co(O_2C_6H_2(t\text{-}Bu)_2)_2(bpy)$ approaches the values found for the bis(semiquinone)cobalt(II) oligomers.[5]

EPR Spectra of $Co(O_2C_6H_2(t\text{-}Bu)_2)_2(bpy)$. As a localized cobalt(III)–semiquinone complex the form of $Co(O_2C_6H_2(t\text{-}Bu)_2)_2(bpy)$ found in the solid state resembles a general class of complexes investigated by Brown,[11] Hendrickson,[12] and Kabachnik.[13] These are typified by the 3,5-di-*tert*-butylsemiquinone complexes $Co(trien)(3,5\text{-}DBSQ)^{2+}$ and Co(salen)(3,5-DBSQ). EPR spectra obtained on free alkyl-substituted semiquinones show strong coupling to protons at the 4 and 5 ring positions due to concentration of spin density within this ring carbon–carbon bond.

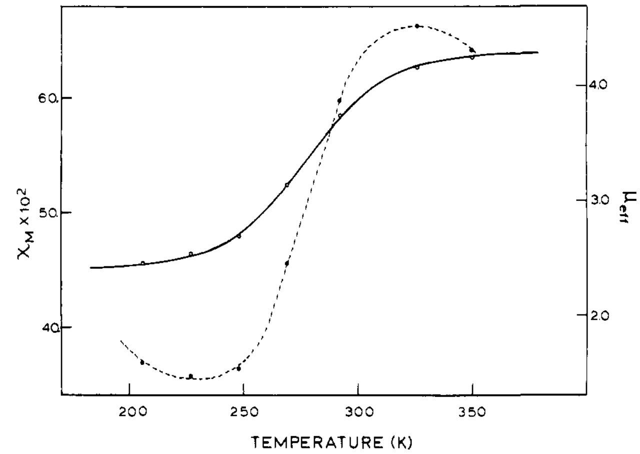

Figure 3. A plot of the solution magnetic susceptibility (dotted line) and magnetic moment of $Co(O_2C_6H_2(t\text{-}Bu)_2)_2(bpy)$ as a function of temperature. Values were obtained in toluene-d_8 by the Evans method.

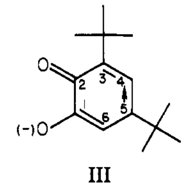

III

Free 3,5-di-*tert*-butylsemiquinone (III) shows coupling of 3.8 G to the ring proton at the 4 position and coupling of 0.3 G to the *tert*-butyl protons at the 5 position.[14] In complexed form it shows basically the same spectrum but with additional hyperfine structure in cases where the metal ion has a nuclear spin. The simple Co(III)–3,5-DBSQ complexes above typically show ring proton hyperfine of 3.5 G and ^{59}Co ($I = {}^7/_2$) coupling of 10–11 G in their solution spectra. As powder samples they have *g* values of 2.00 but show no hyperfine coupling. This is the result we obtain for solid $Co(O_2C_6H_2(t\text{-}Bu)_2)_2(bpy)$. In solution, however, the EPR spectrum is considerably different from the typical cobalt(III)–semiquinone species. In toluene glass at −189 °C and in solution up to a temperature of −40 °C a single resonance is observed which shows no evidence of hyperfine coupling. It is centered at $g = 2.00$ and is approximately twice as broad as the solid-state spectrum. As the temperature of the solution is increased from −40 °C, the intensity of the spectrum begins to decrease without significant broadening. This is shown in Figure 4. At −25 °C indications of ^{59}Co hyperfine appear with a coupling constant of 10.7 G similar to the other cobalt(III)–semiquinone complexes. As the temperature is increased further, intensity

---

(10) Lynch, M.; Hendrickson, D. N., unpublished results.

(11) Wicklund, P. A.; Beckmann, L. S.; Brown, D. G. *Inorg. Chem.* **1976**, *15*, 1996.

(12) Kessel, S. L.; Emberson, R. M.; Debrunner, P. G., Hendrickson, D. N. *Inorg. Chem.*, in press.

(13) Kukes, S. G.; Prokof'ev, A. I.; Masalimov, A. S.; Bubnov, N. N.; Solodovnikov, S. P.; Kabachnik, M. I. *Isv. Akad. Nauk SSSR., Ser. Khim.* **1978**, 1519.

(14) Patai, S., Ed. "The Chemistry of the Quinoid Compounds", Part 1; Wiley: New York, 1974.

continues to decrease but the hyperfine lines become more clearly resolved. At a temperature of 65 °C only the base line is observed. Upon recooling of the solution to −40 °C the original spectrum returned, and similar results can be observed reversibly by either warming or cooling the solution over the temperature range from −40 to +70 °C. Identical results have been obtained in diethyl ether solution[15] and in toluene solutions over the concentration range 10^{-2}–10^{-5} M.

Interligand intramolecular electron-exchange occurring on the EPR time scale could potentially contribute to the temperature dependence of the spectrum. Kabachnik and co-workers have synthesized compounds of phosphorus, silicon, boron, and aluminum which contain both catecholate and semiquinone ligands.[16] A specific example, $P(3,5\text{-DBCat})_2(3,5\text{-DBSQ})$, shows coupling to a single-ring proton at low temperature (−100 °C) and equivalence of all three ligands at higher temperatures. Interligand electron exchange in complexes of this type has been estimated to occur at an approximate rate of 10^9 s^{-1} at 20 °C. This effect may contribute to the difficulty with resolution of the cobalt hyperfine in the present case but should not result in complete loss of the spectrum at higher temperatures. A more plausible explanation is that an EPR inactive species is being formed intramolecularly. This could occur by transfer of an electron from the catecholate ligand to the metal ion producing a Co(II) center (IV), a transformation which is also in accord with the magnetic behavior in solution.

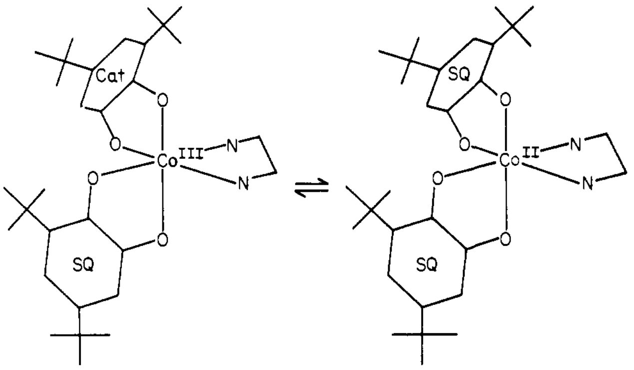

IV

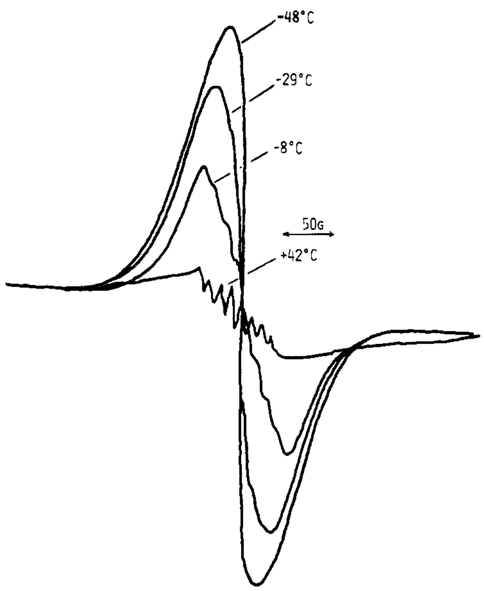

Figure 4. The EPR spectrum of $Co(O_2C_6H_2(t\text{-}Bu)_2)_2(bpy)$ recorded in toluene solution. Greater signal amplitude was required to resolve the +42 °C spectrum. The lower temperature spectra shown were recorded at the same signal amplitude settings.

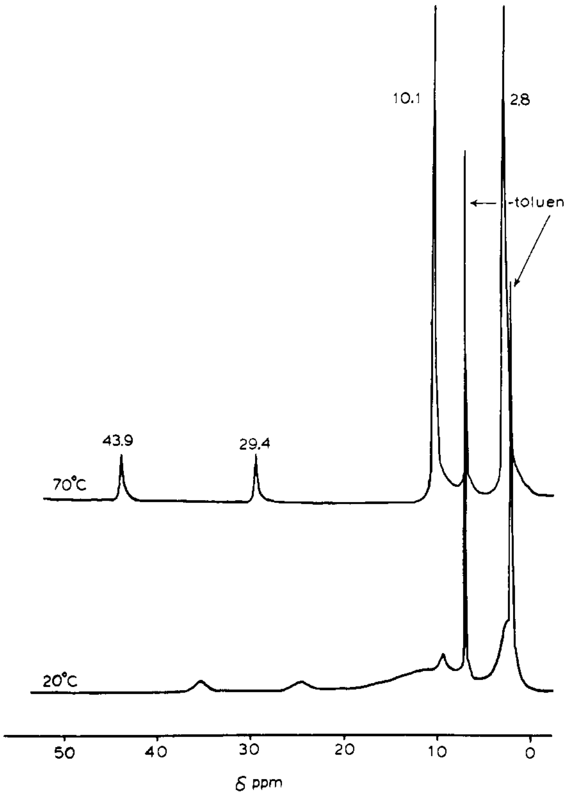

Figure 5. The proton NMR spectrum of $Co(O_2C_6H_2(t\text{-}Bu)_2)_2(bpy)$ recorded in toluene-d_8 solution.

NMR Spectrum of $Co(O_2C_6H_2(t\text{-}Bu)_2)_2(bpy)$. The temperature dependence of the magnetic and EPR experiments suggested a change in electronic structure. Frequently, paramagnetic complexes which fail to give a resolvable EPR signal are amenable to investigation by NMR. Co(trien)(3,5-DBSQ) gives a clear EPR signal but no NMR spectrum. On the other hand (4,7-dimethyl-1,10-phenanthroline)bis(acetylacetonato)cobalt(II) which shows no EPR signal at room temperature shows a clear proton NMR spectrum.

No NMR signal can be resolved for $Co(O_2C_6H_2(t\text{-}Bu)_2)_2(bpy)$ at temperatures below 0 °C. At this temperature five broad resonances appear and become more clearly resolved as temperature is increased to 20 °C. At this temperature the spectrum consists of three resonances of approximately equal intensity at 35.5, 25.4, and 9.5 ppm, with two substantially more intense resonances at 12.3 and 2.7 ppm. At 70 °C the spectrum is well resolved and shows a new broad resonance at 86 ppm with the two downfield resonances now at 43.9 and 29.4 ppm (Figure 5). The two more intense resonances further upfield are quite sharp at this temperature and appear at 10.1 and 2.8 ppm. They are of equal intensity and integrate with a factor of 9:1 with respect to the other four. The resonance formerly at 9.5 ppm becomes more clearly resolved as temperature is increased and appears as a shoulder on the low-field side of the band at 10.1 ppm at 70 °C. We have additionally determined that the temperature dependence of the spectrum is reversible and that it shows no concentration dependence.

The resolution of the NMR spectrum over the temperature range at which the EPR spectrum disappears further suggests a change in charge distribution within the complex, resulting in a Co(II) species. Integration values obtained from the NMR spectrum indicate that the two upfield resonances can be assigned to the quinone *tert*-butyl groups. A rigid octahedral structure for

---

(15) The upper temperature limit for spectral runs recorded in diethyl ether was 30 °C.

(16) (a) Prokof'ev, A. I.; Khodak, A. A.; Malysheva, N. A.; Petrovskii, P. V.; Bubnov, N. N.; Solodovnikov, S. P.; Kabachnik, M. I. *Dolk. Akad. Nauk. SSSR* **1978**, *240*, 92. (b) Prokof'ev, A. I.; Prokof'eva, T. I.; Bubnov, N. N.; Solodovnikov, S. P.; Belostotskaya, I. S.; Ershov, V. V.; Kabachnik, M. I. *Ibid.* **1977**, *234*, 845. (c) Prokof'ev, A. I.; Prokof'eva, T. I.; Bubnov, N. N.; Solodovnikov, S. P.; Belostotskaya, I. S.; Ershov, V. V.; Kabachnik, M. I. *Ibid.* **1977**, *234*, 603.

Table VI. Spectrophotometric Data for $\mathrm{Co(O_2C_6H_2(\mathit{t}\text{-}Bu)_2)_2(bpy)}$

	$\lambda_{\max}$, nm
solid	300 (vs), 360 (sh), 610 (m), 1300 (m)
soln	300 (20 000), 550 (2 000), 610 (2 300),[a] 770 (2 700)[a]

[a] Extinction coefficients were calculated from the 0 °C spectrum for the 610-nm band and from the 60 °C spectrum for the 770-nm band.

either the Co(II) or Co(III) forms of the complex would result in nonequivalence for all four *tert*-butyl groups within the molecule. Optical inversion processes are well-known for Co(II) complexes and at room temperature (4,7-dimethyl-1,10-phenanthroline)-bis(acetylacetonato)cobalt(II) shows equivalence of acac methyl protons.[17] The coordination sphere of the metal in this case is similar to the Co(II) species $\mathrm{Co(3,5\text{-}DBSQ)_2(bpy)}$, and it would not be unusual to observe dynamic behavior for this complex at temperatures above room temperature.

Electronic Spectra of $\mathrm{Co(O_2C_6H_2(\mathit{t}\text{-}Bu)_2)_2(bpy)}$. In the solid state at room temperature the cobalt complex exists as a Co(III) species. In solution the spectral and magnetic properties point to an equilibrium between Co(III) and Co(II) species with the Co(II) complex favored at higher temperatures.

$$\begin{array}{ccc} \mathrm{Co^{III}(3,5\text{-}DBCat)(3,5\text{-}DBSQ)(bpy)} & \rightleftharpoons & \mathrm{Co^{II}(3,5\text{-}DBSQ)_2(bpy)} \\ (t_{2g})^6(e_g)^0(\pi^*_1)^2(\pi^*_2)^1 & & (t_{2g})^5(e_g)^2(\pi^*_1)^1(\pi^*_2)^1 \end{array} \qquad (1)$$

To identify bands in the electronic spectrum which are unique to the two forms of the complex, we recorded spectra over the temperature range from 0 to 60 °C. As a further point of interest, the Co(III) species can be viewed as a mixed-valence complex. Compounds of this form generally consist of related metal ions in different oxidation states bridged by one or more ligands. The ligand bridge frequently permits interaction between metal centers, and Robin and Day[18] have presented a classification scheme based on the extent of interaction. In this regard the Co(III) complex consists of mixed-valence ligands which might be interacting through the bridging-metal center. Such an interaction could give rise to an intervalence-transfer band in the optical spectrum. It was therefore of interest to determine whether the complex shows a low-energy transition which would be indicative of class II behavior.[18]

The high-energy region of the spectrum in toluene solution and in the solid reflectance spectra shows an intense charge-transfer band at 300 nm (Table VI). At lower energy an intense band at 550 nm appears in solution but not in the solid. This band does not show a temperature dependence and appears to be common to both the Co(II) and Co(III) forms of the complex in solution. Two broad bands observed at 610 and 770 nm do show a temperature dependence and appear related to the equilibrium. The 610-nm band decreases in intensity as temperature is increased from 0 °C. It appears in the reflectance spectrum at room temperature and seems associated with the Co(III) form. Catecholate complexes have been reported to typically show ligand to metal charge-transfer bands in this region.[19] The band at 770 nm increases in intensity with an increase in temperature and does not appear in the reflectance spectrum. A similar band is observed for $\mathrm{[Co(3,5\text{-}DBSQ)_2]_4}$ in solution, and this band seems related to the Co(II) form of the complex.

We find nothing further in the near-infrared region for the Co(II) form, but the reflectance spectrum of the species characterized structurally shows an extremely broad band centered at approximately 1300 nm. The band is slightly less intense than the absorption at 610 nm and is roughly 700 nm in breadth. This is most likely the semiquinone–catecholate intervalence band if indeed one exists. Further characterization will be required before we can establish that this is indicative of type II behavior.

Metal–Ligand Electron Transfer in $\mathrm{Co(O_2C_6H_2(\mathit{t}\text{-}Bu)_2)_2(bpy)}$. Intramolecular electron transfer is a fundamental chemical phenomenon and relates specifically to biological redox processes which occur in the chloroplasts and mitochondria. Simple transition-metal complexes which exhibit inner-sphere electron-transfer reactions have been extensively investigated in this context.[1] A particularly interesting class of reactions involving the reduction of Co(III) have appeared which are thought to involve initial reduction of a coordinated organic ligand to a radical anion.[20] This step is then followed by rapid intramolecular, electron transfer to the metal, resulting in the reduced Co(II) product (eq 2).

$$\mathrm{Co(NH_3)_5(L)^{3+} + e^- \rightarrow Co(NH_3)_5(L^-)^{2+} \rightarrow Co^{2+}} \qquad (2)$$

Investigation of transient radical-anion species has been frustrated by their short lifetimes. There has additionally been considerable interest in metal ion reduction reactions involving catechols and hydroquinones.[21] Accurate quantitative data obtained from careful magnetic and spectroscopic investigations of the type described in this report can be used to calculate thermodynamic parameters for cobalt(III) catecholate electron transfer in $\mathrm{Co(O_2C_6H_2(\mathit{t}\text{-}Bu)_2)_2(bpy)}$. These results will appear in a separate publication.

Finally, it is interesting to speculate on the unique factors which contribute to the facility with which metal–ligand electron transfer occurs in this complex. In a simple sense, it relates to the replacement of weak field bridging oxygen donors found in the $\mathrm{[Co(3,5\text{-}DBSQ)_2]_4}$ oligomer with the stronger field bipyridyl ligand. In terms of the electronic structures shown in eq 1, the bipyridyl ligand destabilizes the high-spin Co(II) e_g level, placing one electron in the t_{2g}, resulting in low-spin Co(III), with the second electron populating a quinone π^* level. Unlike the 1,2-dithiolene complexes there is no delocalization within the chelate ring.[22]

Acknowledgments. We thank Professor Gareth Eaton of the University of Denver for his assistance with the EPR experiment. The assistance of Professor Gary Maciel and Dr. James Frye of the NSF Regional NMR Center at Colorado State University is also greatly appreciated. We would additionally like to thank Professor David Hendrickson of the University of Illinois for providing a preprint of ref 12 and for providing information on the magnetic properties of $\mathrm{[Co(3,5\text{-}DBSQ)_2]_4}$. Finally, we acknowledge the National Institutes of Health for support under Grant GM-23386.

Supplementary Material Available: A listing of structure factor amplitudes (9 pages). Ordering information is given on any current masthead page.

---

(17) LaMar, G. N. *J. Am. Chem. Soc.* **1970**, *92*, 1806.

(18) Robin, M.; Day, P. *Adv. Inorg. Chem. Radiochem.* **1967**, *10*, 248.

(19) Henry, R. P.; Mitchell, P. C. H.; Prue, J. E. *J. Chem. Soc. A* **1971**, 3392.

(20) (a) Baxendale, J. H.; Fiti, M. *J. Chem. Soc., Dalton Trans.* **1972**, 1995. (b) Simic, M. G.; Hoffman, M. Z.; Brezniak, N. V. *J. Am. Chem. Soc.* **1977**, *99*, 2166.

(21) (a) Kustin, K.; Nicolini, C.; Topper, D. L. *J. Am. Chem. Soc.* **1974**, *96*, 7416. (b) Reinschmiedt, K.; Sullivan, J. C.; Woods, M. *Inorg. Chem.* **1973**, *12*, 1639. (c) Wells, C. F.; Kuritsyn, L. V. *J. Chem. Soc. A* **1969**, 2930.

(22) McCleverty, J. A. *Prog. Inorg. Chem.* **1968**, *10*, 49.